

A new Monte Carlo method for dynamical evolution of non-spherical stellar systems

Eugene Vasiliev^{1*}

¹*Lebedev Physical Institute, Moscow, Russia*

Accepted 2014 November 4. Received 2014 November 3; in original form 2014 April 1

ABSTRACT

We have developed a novel Monte Carlo method for simulating the dynamical evolution of stellar systems in arbitrary geometry. The orbits of stars are followed in a smooth potential represented by a basis-set expansion and perturbed after each timestep using local velocity diffusion coefficients from the standard two-body relaxation theory. The potential and diffusion coefficients are updated after an interval of time that is a small fraction of the relaxation time, but may be longer than the dynamical time. Thus our approach is a bridge between the Spitzer’s formulation of the Monte Carlo method and the temporally smoothed self-consistent field method. The primary advantages are the ability to follow the secular evolution of shape of the stellar system, and the possibility of scaling the amount of two-body relaxation to the necessary value, unrelated to the actual number of particles in the simulation. Possible future applications of this approach in galaxy dynamics include the problem of consumption of stars by a massive black hole in a non-spherical galactic nucleus, evolution of binary supermassive black holes, and the influence of chaos on the shape of galaxies, while for globular clusters it may be used for studying the influence of rotation.

Key words: galaxies: structure – galaxies: kinematics and dynamics – globular clusters: general – methods: numerical

1 INTRODUCTION

Many problems of stellar dynamics deal with self-gravitating systems which are in dynamical equilibrium, but slowly evolve due to two-body relaxation or some other factor, such as a massive black hole or the diffusion of chaotic orbits. The most general method of studying these systems is a direct N -body simulation, however, in many cases it turns out to be too computationally expensive. Alternative methods, such as Fokker–Planck, gaseous, or Monte Carlo models, have historically been developed mostly for spherical star clusters. In this paper we present a formulation of the Monte Carlo method suitable for non-spherical stellar systems.

The paper is organized as follows. Section 2 reviews the existing simulation methods and outlines the motivation for the proposed new formulation; Section 3 presents the theoretical background of two-body relaxation theory; Section 4 discusses the implementation of the non-spherical Monte Carlo code and Section 5 presents the results of test simulations. Section 6 lists possible applications of the new method and sums up.

2 OVERVIEW OF NUMERICAL METHODS

The development of Monte Carlo methods for simulation of star clusters started in early 1970s with two different approaches, pioneered by Spitzer and Hénon.

In the original formulation of Spitzer & Hart (1971), the motion of test stars in a spherically symmetric potential was followed numerically on the dynamical timescale, and perturbations to the velocity was computed assuming a Maxwellian distribution of background stars (scatterers), with the mean density and velocity dispersion computed in 25 radial bins by averaging over 40 stars in each bin; thus, the test stars were also used for determining the smoothed properties of the field stars. To speed up computation, dependence of velocity diffusion coefficients on the velocity of the test star was ignored (the values corresponded to the average thermal velocity); this simplification was lifted in Spitzer & Thuan (1972). Since perturbations to each star’s velocity are independent of each other, the global conservation of energy is not guaranteed; thus a correction is applied after each timestep which cancels the residual fluctuations. This method became known as the “Princeton” Monte Carlo code (Spitzer 1975).

In another variant of this method, Spitzer & Shapiro (1972) turned to using the diffusion coefficients in energy E

* E-mail: eugvas@lpi.ru

and angular momentum L , averaged over the radial period of the test star. This approach was subsequently developed by Shapiro & Marchant (1978) to study the steady-state solution for the distribution of stars around a massive black hole: the potential was assumed to be dominated by the point mass, the diffusion coefficients in E and L were computed self-consistently from the distribution function $f(E, L)$, which was then adjusted iteratively until convergence. The capture of low angular momentum stars by the black hole was also taken into account, which necessitated a rather complex scheme for choosing the timestep: it was determined by the relaxation time but also required not to miss a potentially disruptive periapsis passage near the black hole. It also had an ingenious scheme for particle cloning (mass refinement) to allow for better sampling of phase-space close to the black hole. Subsequent papers extended the method to self-consistent (rather than point-mass-dominated) potentials (Marchant & Shapiro 1979) and to evolutionary simulation including the heating by the black hole, core collapse, and evaporation (Marchant & Shapiro 1980). This approach has been dubbed the ‘‘Cornell’’ code (Shapiro 1985). More recently, Hopman (2009) and Madigan et al. (2011) have used this formulation to study the dynamics around massive black holes.

At the same time, Hénon (1971a,b) introduced another variant of Monte Carlo method, in which pairs of stars are interacting directly (see also Hénon 1967). Unlike the conventional N -body simulations, these pairwise interactions are computed only between particles that are adjacent in radius. For each pair of interacting particles, their relative velocity is changed by an amount which reproduces statistically the effect of many individual encounters during the same interval of time. The timestep is chosen to be a fraction of the relaxation time T_{rel} , instead of a fraction of the dynamical time T_{dyn} . After each timestep, the stars are assigned new positions (or, rather, radii, since the system is assumed to be spherically symmetric). This method was subsequently improved by Stodólkiewicz (1982), who included a variable timestep (proportional to the radius-dependent T_{rel}), correction of velocities due to the changes in potential after recomputing new positions of particles, continuous stellar mass spectrum, and shock heating due to passages of the globular cluster through the galactic disc. Stodólkiewicz (1986) introduced many other physical ingredients such as stellar evolution, primordial binaries (also studied by Spitzer & Mathieu 1980) and cross-sections for three- and four-body interactions, and stellar collisions.

All presently used codes follow the Hénon’s approach. Since late 1990s, two groups (Giersz 1998; Joshi et al. 2000) have been developing sophisticated codes including much additional physics beyond two-body relaxation: parametrized single and binary stellar evolution (Hurley et al. 2000, 2002; Chatterjee et al. 2010), direct integration of few-body encounters (Giersz & Spurzem 2003; Fregeau & Rasio 2007), accurate treatment of escapers (Fukushige & Heggie 2000). The present versions of these codes are described in Giersz et al. (2013) and Pattabiraman et al. (2013). In these codes, the number of particles in the simulation equals the number of stars in the system under study, which facilitates a correct proportion between various dynamical processes. A third code of the same family was developed by Freitag & Benz (2001, 2002) for studying dense galactic nu-

clei, featuring accurate treatment of loss-cone effects (including a timestep adjustment algorithm similar to that of Shapiro), and a model for physical collisions based on a large library of smooth particle hydrodynamics (SPH) simulations. Table 1 compares the features of various Monte Carlo methods.

In parallel with the Monte Carlo codes, the approach based on direct integration of the Fokker–Planck equation using finite-difference schemes was developed by Cohn (1979, 1980), and later by Takahashi (1993, 1995) and Drukier et al. (1999) for spherical systems. However, it seems to be impractical to extend it beyond two-integral axisymmetric case (Goodman 1983; Einsel & Spurzem 1999; Fiestas & Spurzem 2010), as the method relies on the explicit knowledge of integrals of motion. Another related method is the gaseous model, in which the relaxation is treated using a conductive approximation (Louis & Spurzem 1991; Amaro-Seoane et al. 2004), and which can be combined with Monte Carlo treatment of stellar binaries (Spurzem & Giersz 1996). This approach also was developed in the spherical case only.

With the advent of special-purpose hardware in 1990s, it became possible to perform direct N -body simulations of globular clusters with more than 10^5 stars (Makino 1996; Baumgardt et al. 2004), and a wide range of physics may be added to the dynamical evolution (e.g. Pelupessy et al. 2013). These simulations are also not restricted to any particular geometry, but are very computationally expensive and, as we will show, still practically unsuitable for some classes of problems, in which collisional relaxation should be rather small compared to collisionless effects arising from non-spherical mass distribution. A number of more esoteric approaches have been proposed to combine the flexibility of collisional direct N -body simulations with Fokker–Planck (e.g. McMillan & Lightman 1984), spherical-harmonic expansion (e.g. Hemsendorf et al. 2002), self-similar dynamic renormalization (Szell et al. 2005), or tree-code (McMillan & Aarseth 1993; Fujii et al. 2011; Oshino et al. 2011), none of which apparently gained substantial popularity.

From the side of collisionless simulations of nearly-equilibrium systems, the most relevant for this study are the spherical-harmonic methods (e.g. Aarseth 1967; Clutton-Brock 1973; van Albada & van Gorkom 1977; Hernquist & Ostriker 1992; Meiron et al. 2014). In this approach, the smooth potential of a stellar system is represented as a sum of angular harmonics, with the radial variation of the expansion coefficients being either an explicit function of radius, or another sum over several basis functions. The coefficients of expansion are computed from the spatial distribution of particles, and the equations of motion of particles are governed by the gradients of this smooth potential. In all existing implementations, however, the timestep for particle motion, which is necessarily a small fraction of dynamical time, is also used for updating the coefficients of expansion, thereby imposing random fluctuations on them which effectively create numerical noise comparable to that of more direct N -body methods (Hernquist & Barnes 1990). On the other hand, using some sort of temporal smoothing for the expansion coefficients (proposed by Hernquist & Ostriker 1992, but not tried) might help to reduce the unwanted relaxation considerably

Table 1. Comparison of Monte Carlo methods

Name	Reference	relaxation treatment	timestep	1:1 ^a	BH ^b	remarks
Princeton	Spitzer & Hart (1971); Spitzer & Thuan (1972)	local dif.coefs. in velocity, Maxwellian background $f(r, v)$	$\propto T_{\text{dyn}}$	no	no	
Cornell	Marchant & Shapiro (1980)	dif.coef. in E, L , self-consistent background $f(E)$	indiv., T_{dyn}	no	yes	particle cloning
Hénon	Hénon (1971a)	local pairwise interaction, self- consistent bkgr. $f(r, v_{\parallel}, v_{\perp})$	$\propto T_{\text{rel}}$	no	no	
	Stodólkiewicz (1982) Stodólkiewicz (1986)	Hénon's	block, $T_{\text{rel}}(r)$	no	no	mass spectrum, disc shocks binaries, stellar evolution
	Giersz (1998)	same	same	yes	no	3-body scattering (analyt.)
MOCCA	Hypki & Giersz (2013)	same	same	yes	no	single/binary stellar evol., few-body scattering (num.)
	Joshi et al. (2000)	same	$\propto T_{\text{rel}}(\text{center})$	yes	no	partially parallelized
CMC	Umbreit et al. (2012), Pattabiraman+ (2013)		(shared)	yes	yes	few-body interaction, single/ binary stellar evol., GPU
ME(ssy) ²	Freitag & Benz (2002)	same	indiv. $\propto T_{\text{rel}}$	no	yes	cloning, SPH physical collis.
RAGA	this study	local dif.coef. in velocity, self- consistent background $f(E)$	indiv. $\propto T_{\text{dyn}}$	no	yes	arbitrary geometry

^a One-to-one correspondence between particles and stars in the system

^b Massive black hole in the centre, loss-cone effects

below the discreteness limit, while retaining the ability to follow the slow evolution of a non-spherical system. A similar idea was recently used by Brockamp et al. (2014) in the context of evolution of the population of globular clusters in the galaxy.

The idea to marry the benefits of collisionless expansion codes and collisional Monte Carlo approach has led us to a new formulation of the Monte Carlo method that avoids the restriction to spherical symmetry while retaining the ability to model the two-body relaxation rather faithfully. In essence, it is a successor to the Spitzer's variant of Monte Carlo method, with the orbits of test stars followed in real space in a smooth potential represented by a suitable expansion, and perturbations are applied to particle velocities in accordance with local diffusion coefficients. The new method is dubbed the RAGA code, which stands for "Relaxation in Arbitrary Geometry", but also alludes to slowly developing musical themes in the classical Indian tradition. In addition to this method, we have also implemented a variant of spherical isotropic Fokker–Planck code, similar to that of Cohn (1980), and an orbit-averaged spherical isotropic Monte Carlo code, a simplified version of the method of Marchant & Shapiro (1980), mainly for the purpose of testing the main code. Below, we present a complete mathematical description and test simulations.

3 TWO-BODY RELAXATION

In this section we review the standard two-body relaxation theory as used in our code, referring to Merritt (2013, Chapter 5) for a more complete description. As in most previous studies (the notable exception being Monte Carlo codes based on the Hénon's approach), we consider scattering of

test particles by an isotropic spherically symmetric population of background particles, described by the mass distribution function $f(\mathbf{x}, \mathbf{v}) = f(E)$, where $E \equiv \Phi(\mathbf{x}) + \mathbf{v}^2/2$ is the energy per unit mass. The scattering is described in terms of local (position-dependent) velocity drift and diffusion coefficients (e.g. Merritt 2013, Equations 5.23, 5.55)¹:

$$v\langle\Delta v_{\parallel}\rangle = -\left(1 + \frac{m}{m_{\star}}\right) I_{1/2}, \quad (1a)$$

$$\langle\Delta v_{\parallel}^2\rangle = \frac{2}{3} (I_0 + I_{3/2}), \quad (1b)$$

$$\langle\Delta v_{\perp}^2\rangle = \frac{2}{3} (2I_0 + 3I_{1/2} - I_{3/2}), \quad (1c)$$

where m and m_{\star} are masses of the test and field stars, correspondingly, and

$$I_0 \equiv \Gamma \int_E^0 dE' f(E'), \quad (1d)$$

$$I_{n/2} \equiv \Gamma \int_{\Phi(r)}^E dE' f(E') \left(\frac{E' - \Phi}{E - \Phi}\right)^{n/2}, \quad (1e)$$

$$\Gamma \equiv 16\pi^2 G^2 m_{\star} \ln \Lambda = 16\pi^2 G^2 M_{\text{tot}} \times (N_{\star}^{-1} \ln \Lambda). \quad (1f)$$

These coefficients represent mean and mean-squared changes in velocity per unit time. In the last equation, the term in brackets, or its appropriate generalization for a multimass case, is the only one that depends on N_{\star} (for a given combination of f, Φ). In the Monte Carlo code, we may assign the amplitude of perturbations at will, adjusting this term to a desired number of stars in the target system,

¹ Here, we make the usual Chandrasekhar's approximation by assuming that the drift (friction) term is determined only by background stars that move more slowly than the test star. One should keep in mind that in some situations this approximation breaks down (Antonini & Merritt 2012).

which needs not be related to the number of particles in the simulation. In Hénon’s formulation, the particles were called “superstars”, and their masses were a fixed multiple of actual stellar mass; contemporary codes usually have 1:1 correspondence between the particle and star mass, which facilitates the introduction of additional physical processes such as binary–single star scattering cross-section. In our approach, we do not require a fixed proportionality coefficient between the particle and star masses – particles are just mass tracers and not actual stars, and the relaxation is determined by the smooth distribution function and not by discrete encounters.

In the rest of this section, we focus on the isotropic spherically symmetric case, which is used in the auxiliary codes, while the treatment of relaxation in the main RAGA code relies only on the velocity diffusion coefficients (1), with some secondary routines using the orbit-averaged energy diffusion coefficient. Even in the spherical case, it is not necessary that the distribution of stars is isotropic: Marchant & Shapiro (1980) worked in a two-dimensional $\{E, L\}$ phase-space, but retained the isotropic background approximation.

Local drift and diffusion coefficients in energy are

$$\langle \Delta E \rangle = v \langle \Delta v_{\parallel} \rangle + \frac{1}{2} \langle \Delta v_{\parallel}^2 \rangle + \frac{1}{2} \langle \Delta v_{\perp}^2 \rangle = I_0 - I_{1/2}, \quad (2a)$$

$$\langle \Delta E^2 \rangle = v^2 \langle \Delta v_{\parallel}^2 \rangle = \frac{2}{3} v^2 (I_0 + I_{3/2}). \quad (2b)$$

The isotropic Fokker–Planck equation² describing the relaxation in energy has two forms. The first is more convenient for Monte Carlo simulations, the second (flux-conservative) is more suitable for solving the Fokker–Planck equation on a grid. Define $N(E) \equiv g(E)f(E)$ to be the mass density of stars per unit energy, where the density of states

$$g(E) \equiv 16\pi^2 \int_0^{r_{\max}(E)} dr r^2 v = 4\pi^2 L_{\text{circ}}^2(E) P(E), \quad (3)$$

$r_{\max}(E)$ is the apocentre radius of a radial orbit with energy E (so that $\Phi(r_{\max}(E)) = E$), $L_{\text{circ}}(E)$ is the angular momentum of a circular orbit with the given energy, and $P(E) \equiv 2 \int_0^{r_{\max}} dr/v$ is the period of a radial orbit (time needed to complete one oscillation in the radial direction). Ignoring the time dependence of potential, the Fokker–Planck equation reads

$$\frac{\partial N(E)}{\partial t} = -\frac{\partial}{\partial E} (N(E) \langle \Delta E \rangle_{\text{av}}) + \frac{1}{2} \frac{\partial^2}{\partial E^2} (N(E) \langle \Delta E^2 \rangle_{\text{av}}), \quad (4)$$

with $\langle \dots \rangle_{\text{av}}$ being the averaged values of corresponding quantities over the phase volume accessible to the orbit. For the spherical case, these averages are given by

$$\langle \dots \rangle_{\text{av}} = \frac{16\pi^2}{g(E)} \int_0^{r_{\max}(E)} dr r^2 v \langle \dots \rangle. \quad (5)$$

The calculation of averaged coefficients for energy is made easier by introduction of a few auxiliary functions:

$$h(E) \equiv \frac{16\pi^2}{3} \int_0^{r_{\max}(E)} dr r^2 v^3 = \int_{\Phi(0)}^E dE' g(E'), \quad (6)$$

² It should be more appropriately called the generalized Landau equation, as it is a nonlinear integro-differential equation containing the unknown distribution function in the diffusion coefficients as well (Chavanis 2013).

$$K_1(E) \equiv \int_E^0 dE' f(E'), \quad (7a)$$

$$K_g(E) \equiv \int_{\Phi(0)}^E dE' f(E') g(E'), \quad (7b)$$

$$K_h(E) \equiv \int_{\Phi(0)}^E dE' f(E') h(E'). \quad (7c)$$

The function $K_g(E)$ measures the mass of stars having energy below E , while K_h does the same for kinetic energy (up to a factor 3/2). These three functions, together with $h(E)$ and its derivative $g(E)$, can be tabulated for the given combination of $f(E)$ and $\Phi(r)$ and cheaply interpolated to obtain the drift and diffusion coefficients:

$$\langle \Delta E \rangle_{\text{av}} = \Gamma [K_1(E) - K_g(E)/g(E)], \quad (8a)$$

$$\langle \Delta E^2 \rangle_{\text{av}} = 2\Gamma [K_1(E)h(E) + K_h(E)]/g(E). \quad (8b)$$

4 THE NEW MONTE CARLO METHOD

Having reviewed the theory of two-body relaxation, we now describe the implementation of the new Monte Carlo code. In the present form, it is hardly suitable for realistic dynamical simulations of star clusters, lacking many sophistications found in other existing codes. We assume a population of identical single stars, neglect the dynamical influence of binaries and stellar evolution, and do not consider external tidal forces that would lead to escape of stars from the systems. Most of these ingredients are not difficult to add; the purpose of this paper is to show the feasibility and benefits of non-spherical dynamical Monte Carlo modelling.

The main advantage of position-dependent diffusion coefficients in velocity is that one may apply them to orbits of arbitrary shape, not restricted to spherical symmetry. For a very general and flexible representation of the potential, we use two variants of spherical-harmonic expansions implemented in the publicly available SMILE software (Vasiliev 2013): basis-set and spline expansions. In both cases, the angular dependence of the potential is given by spherical harmonics, while for the radial part either a finite sum over a particular set of basis functions with adjustable coefficients is used, or the radial dependence of each spherical harmonic is represented with a spline function. This representation typically uses 10 – 20 radial terms, and the order of the angular expansion $l_{\max} = 4 - 6$ is sufficient for moderately flattened systems (with major to minor axis ratio $\lesssim 2$). We refer to the appendix of the above paper for more details. Throughout this section, we denote the actual non-spherical potential in which the particles move as $\tilde{\Phi}(\mathbf{r}) \equiv \tilde{\Phi}(r, \theta, \phi)$, and its associated density as $\tilde{\rho}$, while the quantities from an equivalent spherical system, approximating the actual density profile (see below), are without tildes.

The evolution of the N -body system is followed through a series of “episodes” – intervals of time T_e during which all particles move along their orbits independently from each other (thus the computation of orbits is trivially parallelized). At the end of an episode, the global state of the system (the potential and the diffusion coefficients) is updated using the orbits of particles during the episode: each orbit is sampled with N_{samp} points (position and velocity of

the given particle at regular intervals of time). If $N_{\text{samp}} \gg 1$, this increases the effective number of particles used in recomputing the potential and distribution function, reducing the discreteness noise.

The motion of particles in the smooth potential of the entire system is computed using one of the ODE integrators from SMILE: a standard eighth-order Runge–Kutta method DOP853 (Hairer et al. 1993), or several other methods from the ODEINT package (Anhert & Mulansky 2011). After each timestep, the perturbations to the velocity are computed as

$$\Delta v_{\parallel} = \langle \Delta v_{\parallel} \rangle \Delta t + \zeta_1 \sqrt{\langle \Delta v_{\parallel}^2 \rangle \Delta t}, \quad (9a)$$

$$\Delta v_{\perp} = \zeta_2 \sqrt{\langle \Delta v_{\perp}^2 \rangle \Delta t}, \quad (9b)$$

where ζ_1, ζ_2 are two independent random numbers with standard normal distribution, Δt is the timestep adjusted internally in the ODE integrator, and the diffusion coefficients are given by (1). While there are more sophisticated methods for dealing with stochastic differential equations (e.g. Kloeden & Platen 1995), we used the simplest explicit order 0.5 method for the stochastic part in combination with a high-order method for the deterministic part, which enables to follow the unperturbed trajectories with a great accuracy. We have checked that the choice of the integration method and the timestep criterion for the ODE integrator do not affect the statistical properties of accumulated changes in energy and angular momentum after a given interval of time $\gtrsim T_{\text{dyn}}$. Typically, the ODE integrator places several tens of timesteps and reaches the energy conservation error of better than 10^{-8} per T_{dyn} for an unperturbed orbit. A similar approach (interleaving the evolution in the smooth field with the two-body perturbations) was used by Weinberg & Katz (2007) for studying the effect of noise on the behaviour of near-resonant orbits in spiral galaxies, and by Johnston et al. (1999) for simulating the tidal mass-loss from galactic satellites (they used diffusion coefficient computed under the approximation of locally Maxwellian velocity distribution).

The treatment of relaxation relies on the local diffusion coefficients (1) which are computed using an isotropic spherically symmetric equivalent of the system under study. This approximation (in particular, assumption of isotropy of velocities of background stars) is typical in the relaxation theory, however it could break down in a strongly non-spherical or anisotropic system. A modification of the present approach could be adopted for a rotating stellar system, assuming isotropic velocity distribution in the corotating frame (Goodman 1983; Einsel & Spurzem 1999); we have not implemented it here.

At the beginning of the simulation, the equivalent spherical system is constructed by averaging the density profile $\bar{\rho}(r, \theta, \phi)$ of the actual model over angles θ, ϕ , retaining only the radial dependence of mass profile $M(r)$. Then the associated spherically symmetric potential $\Phi(r)$ is computed, along with the isotropic distribution function $f(E)$ from the Eddington equation. Later in the course of simulation, both the spherically symmetric mass profile which produces the associated potential, and the distribution function, are updated directly from the particle orbits (using points sampled during the episode). Both the mass profile and the distribution function are constructed using a penalized

spline smoothing approach (Green & Silverman 1994), similar to the one employed in the MKSPHERICAL program from SMILE. For the latter, we first compute $N(E) dE$ from the positions and velocities of sample points, using the spherically symmetric potential $\Phi(r)$, then smooth it, and finally $f(E)$ is obtained by dividing the smoothed $N(E)$ by the density of states $g(E)$ (Equation 3), again from the equivalent spherical system.

After calculating the distribution function $f(E)$, we compute the functions $I_0, I_{n/2}$ that enter the definition of diffusion coefficients (1). They depend on the energy of the test star E and the (spherical) potential at the given position $\Phi(r)$, and we store the pre-computed functions on a grid in $\{E, \Phi\}$ space. In the course of orbit integration, the actual values of these functions are efficiently obtained from two-dimensional interpolation. For the given position and velocity of the particle in the actual (non-spherical) potential, the value of potential Φ and energy E used as the arguments of these functions are taken from the spherically symmetric potential $\Phi(r)$ at the given position. Thus, the actual potential $\Phi(r, \theta, \phi)$, responsible for the regular motion, and the diffusion coefficients for the stochastic perturbations, are computed using slightly different methods – one for the actual system, the other for its spherical equivalent. The small incoherence amounts to the approximation of spherical isotropic scattering background, as used in most previous studies, and is believed not to cause substantial distortions to the dynamics. Note that the test stars themselves do not need to be isotropic in velocity – this assumption is only used for the background stars.

In contrast with the Hénon’s formulation of Monte Carlo method, in which the energy is conserved by pairwise interactions (but not by the potential update; see Stodólkiewicz (1982) for an amendment), the Spitzer and Shapiro’s variants do not have this property intrinsically: each particle randomly walks in energy independently from others. To correct for this, at the end of the episode we compute the accumulated energy error and distribute it between particles, in proportion with their average diffusion coefficient $\sqrt{\langle \Delta E^2 \rangle_{\text{av}}}$ (8) during this episode. This is slightly different from the correction method employed by Marchant & Shapiro (1980) and primarily applies the correction to those particles that have experienced the largest diffusion. We compensate the energy error by correcting the particle velocity at the end of the episode, changing its magnitude (but not direction) by a necessary amount.

The true non-spherical potential used to compute particle motion is also updated at the end of an episode, using the same sampling points (N_{samp} per orbit) collected during the episode. As already mentioned, $N_{\text{samp}} \gg 1$ reduces discreteness noise in the potential expansion coefficients; furthermore, if $T_e \gg T_{\text{dyn}}(E)$ for most of the orbits in the system, each particle completes many periods during one episode, thus again smoothing out fluctuations. This is, in essence, the “temporal smoothing” proposed by Hernquist & Ostriker (1992) but apparently never used before. (Note that there exist simulation methods that rely on “orbit–orbit”, as opposed to “particle–particle” interactions, which are used for stars on near-Keplerian orbits around a massive black hole (Touma et al. 2009; Kocsis & Tremaine 2014; Hamers et al. 2014); these approaches hardly can be

generalized for arbitrary potentials not dominated by a single point mass).

The energies of particles also need to be corrected after reinitialization of the potential, to account for the time dependence of the potential. We adopt the method used by Stodólkiewicz (1982) and Giersz (1998), which states that the energy correction for a given particle is

$$\Delta \tilde{E}_i = \frac{1}{2} \left[\Delta \tilde{\Phi}(\mathbf{r}_{i,\text{old}}) + \Delta \tilde{\Phi}(\mathbf{r}_{i,\text{new}}) \right], \quad (10)$$

where $\mathbf{r}_{i,\text{old}}$ and $\mathbf{r}_{i,\text{new}}$ are particle positions at the beginning and end of the episode, and $\Delta \tilde{\Phi}(\mathbf{r}) \equiv \tilde{\Phi}_{\text{upd}}(\mathbf{r}) - \tilde{\Phi}_{\text{old}}(\mathbf{r})$ is the difference between the updated potential and the old one (used during the episode). In these papers, this correction could be applied directly to the particle's energy, while in our case we are again forced to attribute it to the kinetic energy only. More specifically, the updated velocity after the correction is related to the “new” velocity (at the end of the episode but before the correction) by

$$\begin{aligned} \frac{v_{i,\text{upd}}^2}{2} + \tilde{\Phi}_{\text{upd}}(\mathbf{r}_{i,\text{new}}) &= \frac{v_{i,\text{new}}^2}{2} + \tilde{\Phi}_{\text{old}}(\mathbf{r}_{i,\text{new}}) + \Delta \tilde{E}_i, \\ v_{i,\text{upd}}^2 - v_{i,\text{new}}^2 &= \Delta \tilde{\Phi}(\mathbf{r}_{i,\text{old}}) - \Delta \tilde{\Phi}(\mathbf{r}_{i,\text{new}}). \end{aligned} \quad (11)$$

As shown by Stodólkiewicz (1982), this correction ensures the conservation of total energy of the system $\mathcal{E} \equiv \sum_i m_i \left[v_i^2/2 + \tilde{\Phi}(r_i)/2 \right]$ in his case. Indeed,

$$\mathcal{E}_{\text{upd}} - \mathcal{E}_{\text{old}} = \sum_i m_i \left[\frac{v_{i,\text{upd}}^2}{2} + \frac{\tilde{\Phi}_{\text{upd}}(\mathbf{r}_{i,\text{new}})}{2} - \frac{v_{i,\text{old}}^2}{2} - \frac{\tilde{\Phi}_{\text{old}}(\mathbf{r}_{i,\text{old}})}{2} \right] =$$

$$\sum_i m_i \left[\frac{v_{i,\text{new}}^2}{2} + \tilde{\Phi}_{\text{old}}(\mathbf{r}_{i,\text{new}}) \right] - \quad (12a)$$

$$\sum_i m_i \left[\frac{v_{i,\text{old}}^2}{2} + \tilde{\Phi}_{\text{old}}(\mathbf{r}_{i,\text{old}}) \right] + \quad (12b)$$

$$\sum_i m_i \frac{\tilde{\Phi}_{\text{upd}}(\mathbf{r}_{i,\text{old}}) - \tilde{\Phi}_{\text{old}}(\mathbf{r}_{i,\text{new}})}{2}. \quad (12c)$$

The first two terms (12a) and (12b) represent the sum of energies of all particles, which is conserved by the relaxation step followed by the cancellation of fluctuations described above. The last term (12c) also should tend to zero in the continuum limit (Stodólkiewicz 1982, Eq.37). However, his proof is valid only if the updated potential is computed from the positions of particles at the end of the episode; if we use $N_{\text{samp}} > 1$ sampling points, this is no longer true. Therefore, we compute the last term explicitly, and cancel the total energy error $\mathcal{E}_{\text{upd}} - \mathcal{E}_{\text{old}}$ by distributing it between all particles.

In all these correction steps, we can only attribute the energy error to the kinetic energy by changing the magnitude of particle velocities. This might introduce some bias, as the energy excess/deficit is attributed entirely to the kinetic energy (and furthermore, if the energy needs to be subtracted from a particle happened to be around its turning point, the velocity may be too small to allow it, in which case it remains undercorrected), but it is the simplest practical way of cancelling the energy errors. We do not apply a similar correction to angular momentum fluctuations, as they remain small ($\sim N^{-1/2}$) and do not have a preferred sign (however, we only considered systems with zero total

angular momentum and cannot be sure that there will be no secular drift in angular momentum if it was non-zero initially).

For the two auxiliary methods used for comparison – spherical isotropic Fokker–Planck and Monte Carlo codes – there is no need to follow orbits in space, only the evolution of distribution function $f(E)$ and its associated potential–density pair $\rho(r), \Phi(r)$. In the finite-difference Fokker–Planck scheme, $f(E)$ is sampled on a non-uniform grid in E , and a flux-conservative implicit Chang & Cooper (1970) scheme is used (see Park & Petrosian 1996, for a comparison of numerical methods). In the Monte Carlo scheme, the distribution function is sampled by discrete particles with energies E_i , and during each episode, each particle performs one or more Monte Carlo steps with timestep Δt , according to

$$\Delta E_i = \langle \Delta E \rangle_{\text{av}} \Delta t + \zeta \sqrt{\langle \Delta E^2 \rangle_{\text{av}} \Delta t}, \quad (13)$$

with ζ being a random number with standard normal distribution, and the diffusion coefficients given by (8). The timestep is assigned so that the expected change in energy does not exceed $\eta \min(|E|, E - \Phi(0))$, with the tolerance parameter $\eta \simeq 0.2$. When all particles have completed the episode, a new distribution function is computed in the same way as in the full RAGA code (i.e., using penalized spline smoothing).

The spherical potential is updated after the new distribution function has been computed, by using the following relation for the density:

$$\rho(r) = 4\pi \int_{\Phi(r)}^0 dE f(E) \sqrt{2(E - \Phi(r))}, \quad (14)$$

and then the Poisson equation for the potential. Followed by recomputation of the potential, the distribution function must be changed adiabatically, which is easiest to achieve by expressing it in terms of the phase volume h (6) instead of E , and then transforming back using the updated potential. As the equation (14) contains the unknown potential itself, it should be applied iteratively until convergence, while keeping $f(h(E))$ constant at each iteration while E changes. In practice, we found that for the Fokker–Planck method one iteration is sufficient, provided that timestep for the update is small enough; for the spherical Monte Carlo code, we perform several iterations to reduce the impact of fluctuations of potential at origin, where the number of particles is small. For a simulation of a deep collapse, the accumulated energy error is $\sim 1 - 2\%$.

5 TESTS

In this section, we describe several test problems for the new Monte Carlo method. First, we demonstrate that temporal smoothing does help to reduce energy exchange between particles due to fluctuations of the potential to a negligible level, compared with the typical two-body relaxation rates. Then, we perform two standard tests: the core collapse of a Plummer sphere, and the growth of a Bahcall–Wolf cusp around a massive black hole. Finally, we consider the shape evolution of a triaxial model with a black hole.

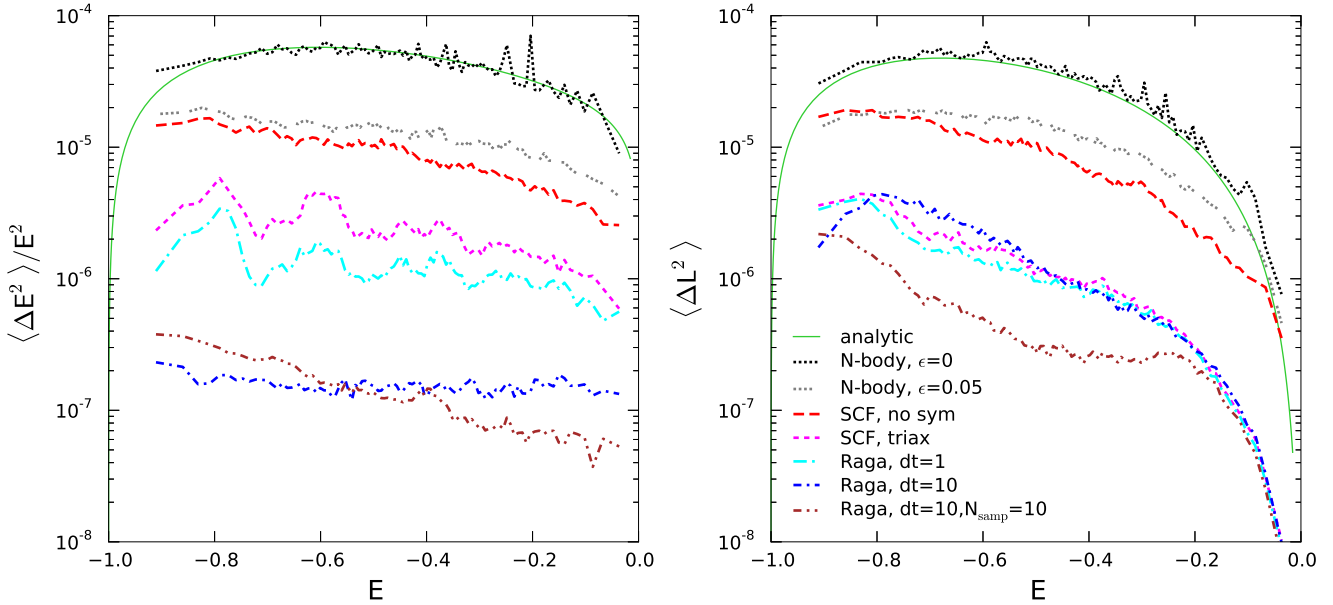


Figure 1. Comparison of energy (left) and angular momentum (right) diffusion rates as functions of energy, for various methods. The system under study is a spherical Plummer model with $N = 10^5$ particles, evolved for $T = 100$ time units (roughly 1/20 of the half-mass relaxation time). Plotted are mean squared changes in particle energy and angular momentum per unit time, averaged over 10^3 particles in 100 energy bins. Energy diffusion coefficient is divided by squared energy for convenience. The solid lines are the analytically computed diffusion coefficients, assuming the value of Coulomb logarithm $\ln \Lambda = 9.3$. Dotted lines are the results of a direct N -body simulation, which agree well with the analytical predictions. Dashed lines are from SCF simulations with $n_{\max} = 15$ radial and $l_{\max} = 4$ angular coefficients: top is for the simulation retaining all coefficients, bottom is for the one with imposed triaxial symmetry (retaining only cosine coefficients with even l, m). The timestep for the SCF simulation is $1/32$, or $\sim 10^{-2}$ dynamical times at the centre. Other lines are for the Monte Carlo code with relaxation switched off, and using the same potential representation (Hernquist–Ostriker basis set with the same number of coefficients and imposed triaxial symmetry), but different settings for update interval: 1 time unit, 10 time units (longer than the dynamical time for most particles), and 10 time units with 10 sampling points for each particle during this interval. Clearly, introduction of temporal softening (in terms of longer update interval) and increase of the number of sampling points decreases the fluctuations of the potential and reduces the diffusion of energy and angular momentum by as much as two orders of magnitude, with respect to the direct N -body simulation. A Monte Carlo simulation with relaxation included (not shown) produces the diffusion rate in very close agreement with the analytic predictions.

5.1 Temporal smoothing test

In this test we consider the relaxation rate of a spherical Plummer model, evolved with different methods: N -body simulation with a direct-summation code, self-consistent field (SCF) method, and the RAGA code with relaxation turned off. The goal is to demonstrate that temporal smoothing does substantially reduce the energy and angular momentum relaxation rate, compared to more direct simulation methods. We take an $N = 10^5$ Plummer model with total mass and scale radius both equal to 1 N -body units, and evolve it for $T = 100$ time units, or roughly 1/20 of the half-mass relaxation time. To measure the relaxation rate, we record the changes in energy and angular momentum of individual particles, average them over particles in each of 100 bins sorted in energy, and fit a linear regression to the squared difference between initial and current values of E and L as functions of time (see Theuns (1996) for a somewhat different method of estimating the relaxation rate). The coefficient of this regression represents the diffusion coefficient $\langle \Delta E^2 \rangle_{\text{av}}$ (8) and a similarly computed coefficient for L . We have checked that the growth of ΔE^2 and ΔL^2 is indeed close to linear in time, with occasional fluctuations.

For the conventional N -body simulation we

use the GPU-accelerated direct-summation code ϕ GRAPE (Harfst et al. 2007) with the SAPPORO library (Gaburov et al. 2009). Figure 1 demonstrates that the theoretically computed diffusion rates agree very well with the measured values from the direct N -body simulation without softening, using the standard value of the Coulomb logarithm $\ln \Lambda = \ln 0.11 N \approx 9.3$ (Giersz & Heggie 1994). In collisionless simulations, softening is used to reduce the graininess of the potential; we have run another simulation with $\epsilon = 0.05$, which is close to the optimal value for this N (Merritt 1996; Athanassoula et al. 1998) and reduces the relaxation rate by a factor of few (Theis 1998). The other, “indirect” N -body simulation method that we used was the SCF method of Hernquist & Ostriker (1992), employed in two regimes: in the first case we used all expansion coefficients ($n_{\max} = 15$ radial and $l_{\max} = 4$ angular terms), in the second – retained only the non-zero terms for a triaxially symmetric model (that is, cosine terms with even l and m). Figure 1 shows that the SCF method demonstrates a several times lower rate of diffusion than a direct N -body simulation, when using all coefficients, and a further factor of few lower rate for a model with imposed triaxial symmetry. This is not unexpected, given that the potential in the SCF method is fairly smooth, but the

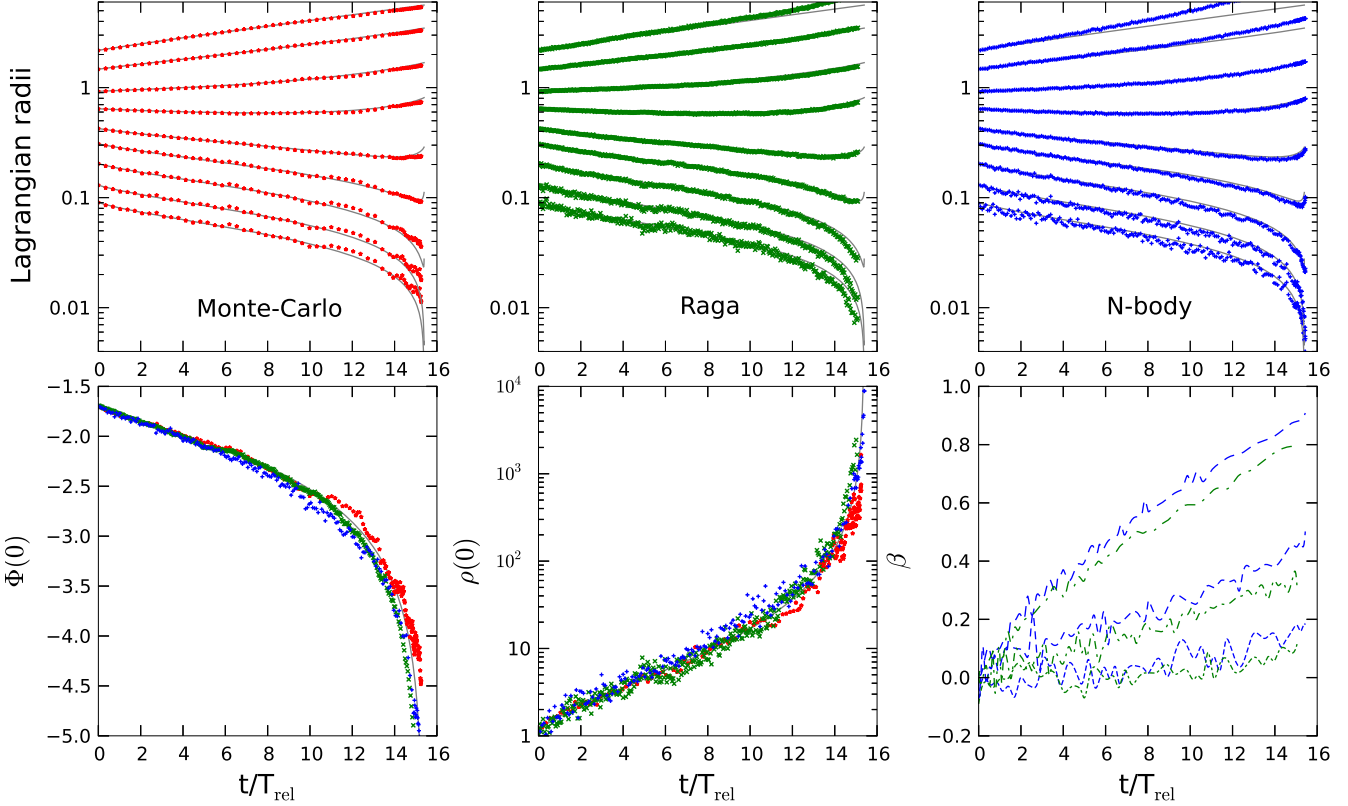


Figure 2. Comparison of time evolution of various quantities in a simulation of a Plummer model undergoing core collapse, performed with the spherical Fokker–Planck (grey lines) and Monte Carlo (red stars) methods, the RAGA code (green diagonal crosses) and a direct N -body simulation (blue horizontal crosses). Time is expressed in units of half-mass relaxation time ($T_{\text{rel,h-m}} \equiv 0.093 N / \ln \Lambda$), with the adopted value $\ln \Lambda = 6.5$ for the N -body simulation being lower than the usually employed $\ln \Lambda = \ln 0.11 N \approx 7.5$, thus bringing the collapse time in this particular simulation into better agreement with the Fokker–Planck simulation.

Top row: Lagrangian radii containing the fraction of mass equal to 0.0035, 0.01, 0.035, 0.1, 0.2, 0.4, 0.6, 0.8, 0.9 (from bottom to top). Bottom left: the value of potential in the centre (starting from $-16/(3\pi) \approx -1.7$). Bottom centre: central density. Bottom right: velocity anisotropy parameter $\beta \equiv 1 - \frac{\sigma_t^2}{2\sigma_r^2}$ (where σ_t and σ_r are the transversal and radial velocity dispersions), evaluated in three shells, enclosed by Lagrangian radii containing 45 to 50, 70 to 75, and 90 to 95% of total mass (from bottom to top). Dashed lines are from N -body simulation and dot-dashed – from the RAGA simulation (the other two methods assume isotropic velocity).

reduction of relaxation rate is limited by the fluctuations in the potential arising from frequent updates in the coefficients, as the update interval is equal to the timestep of equations of motion (taken to be a small fraction ($\sim 10^{-2}$) of the dynamical time in centre), and is comparable to the reduction due to softening in a direct N -body simulation (Hernquist & Barnes 1990). It can further be improved by a factor of few by using a carefully constructed basis set (Weinberg 1996).

On the other hand, if we allow for less frequent updates in the potential while retaining the high accuracy in integrating the equations of motion, then the relaxation rate may be reduced even further, as shown by the simulations of RAGA code with longer update intervals (we checked that running it with the same timestep as the SCF code produced identical results to the latter). Increasing the number of sampling points N_{samp} for each particle per episode reduces the fluctuations even further. Overall, for this model we attained a factor of hundred reduction in the relaxation rate, limited only by the update frequency: if the system needs to be simulated for a time substantially shorter than

its relaxation time (or the time for any other effect to change its structure significantly), then the potential update may be switched off altogether, entirely eliminating this source of unwanted fluctuations. On the other hand, the necessary level of relaxation is readily restored by adding the stochastic two-body perturbation term to the equations of motion. We have checked that this produced essentially the same total relaxation as the direct N -body simulation, if the amplitude of perturbation term in Equation (1f) was assigned accordingly, using the same values of N and Λ .

5.2 Core collapse test

Self-gravitating systems are known to have negative specific heat and exhibit the phenomenon of core collapse (Heggie & Hut 2003, Chapter 18). The easiest and probably most studied example is that of a Plummer sphere composed of equal-mass particles, for which various studies based on isotropic Fokker–Planck method have found the core collapse time to be ≈ 15 initial half-mass relaxation times $T_{\text{rel,h-m}}$ (e.g. Spitzer & Shull 1975; Cohn 1980;

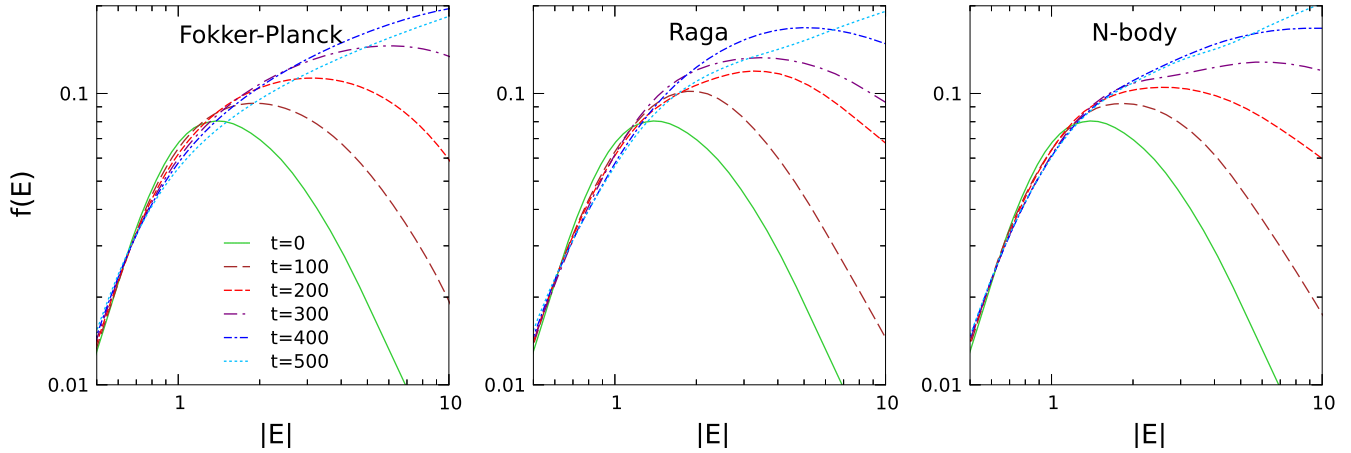


Figure 3. Evolution of distribution function in a system with a central black hole: left panel – Fokker–Planck, centre – RAGA, right – N -body simulation. The system is a $N = 32000$ realization of a spherical $\gamma = 1$ Dehnen model with the black hole mass $M_{\bullet} = 0.1$ of the total mass in stars. The Bahcall–Wolf cusp with the density profile $\rho \propto r^{-7/4}$, corresponding to the distribution function $f(E) \propto |E|^{1/4}$, develops after roughly 400 time units, or roughly $0.2 T_{\text{rel}}(r_m)$ (or one T_{rel} at a radius $\sim 0.2r_m$, where the relaxation time is shortest initially). We scaled the relaxation rate using the value of Coulomb logarithm $\ln \Lambda = \ln M_{\bullet}/m_{\star} \approx 8$. Different codes show a rather good agreement in the evolution of distribution function towards the steady-state solution.

Takahashi 1993; Quinlan 1996). As discussed in the latter paper, a constant value of Coulomb logarithm overestimates the relaxation rate in the centre at later stages of core collapse, as the effective number of stars in the core decreases; anisotropic models also tend to have longer collapse times (e.g. Takahashi 1995).

For this test, we set up an $N = 16384$ Plummer model in the virial units (with the scale radius set to $3\pi/16$). In the calibration N -body run, performed by the same code ϕ GRAPE, the moment of collapse corresponds to $T_{\text{coll}} \approx 3630$ time units, in agreement with other N -body studies (Makino 1996; Baumgardt et al. 2003). With the standard choice of Coulomb logarithm $\ln \Lambda \approx 7.5$ this corresponds to $17.8 T_{\text{rel,h-m}}$; for the purpose of comparison with the isotropic Fokker–Planck and Monte Carlo simulations we have used a smaller value $\ln \Lambda = 6.5$, which brings the collapse time in this particular simulation into better agreement with other methods.

Next we have run spherical isotropic Fokker–Planck and Monte Carlo codes, as well as the full RAGA code. The Fokker–Planck simulation was taken as reference, with the time until core collapse being $15.4 T_{\text{rel,h-m}}$, in excellent agreement with other studies. Figure 2 shows the evolution of various quantities (Lagrangian radii, central density and potential, and velocity anisotropy) in different simulations. Overall, the agreement between various methods is fairly good, at least until the central density increases by a factor of 10^3 ; closer to the time of collapse, we do not expect either method to be reliable without taking into account the binary formation and heating and other phenomena beyond two-body relaxation. By the end of the simulation, the accumulated energy error was around 2%.

5.3 Bahcall–Wolf cusp growth test

The density profile around a point mass (massive black hole) has a steady-state power-law solution of the Fokker–

Planck equation, known as the Bahcall & Wolf (1976) cusp: $\rho(r) \propto r^{-7/4}$ for a single-component star cluster. Dynamical models starting from different initial conditions tend to develop the cusp at radii smaller than $r \sim 0.2r_m$, where the influence radius of the black hole r_m contains the mass in stars equal to twice the black hole mass. This has been observed both in Fokker–Planck models (e.g. Cohn & Kulsrud 1978; Merritt 2009) and in N -body simulations (Preto et al. 2004; Baumgardt et al. 2004; Merritt & Szell 2006). As the relaxation time in the Newtonian potential of the central point mass is proportional to $\rho^{-1}(r)r^{-3/2}$, if the initial density profile was shallower than $r^{-3/2}$, then the cusp grows from outside in.

We have set up a spherical Dehnen (1993) model with $\gamma = 1$, $N = 32000$ and a central black hole with mass $M_{\bullet} = 0.1$ of the total mass in stars, drawing particle positions and velocities from a self-consistent isotropic distribution function (e.g. Tremaine et al. 1994), computed numerically from the Eddington’s formula, using the MKSPHERICAL program from SMILE. Then, we evolved the model until it developed the steady-state Bahcall–Wolf profile. The N -body simulation used a version of code with chain regularization (ϕ GRAPEch, Harfst et al. 2008). In the Fokker–Planck model we adopted a zero-flux boundary condition at the black hole. Figure 3 shows the gradual evolution of the distribution function towards the $|E|^{1/4}$ solution. The agreement between Fokker–Planck, Monte Carlo and N -body simulations is again quite good.

5.4 Shape evolution test

Up to now we have considered spherical systems, to facilitate comparison between various methods. We now turn to the unique feature of RAGA code, namely the ability to simulate systems of arbitrary geometry. For this test, we take a triaxial $\gamma = 1$ Dehnen model with axis ratio of $1 : 0.8 : 0.5$ and a central black hole with mass $M_{\bullet} = 0.01$

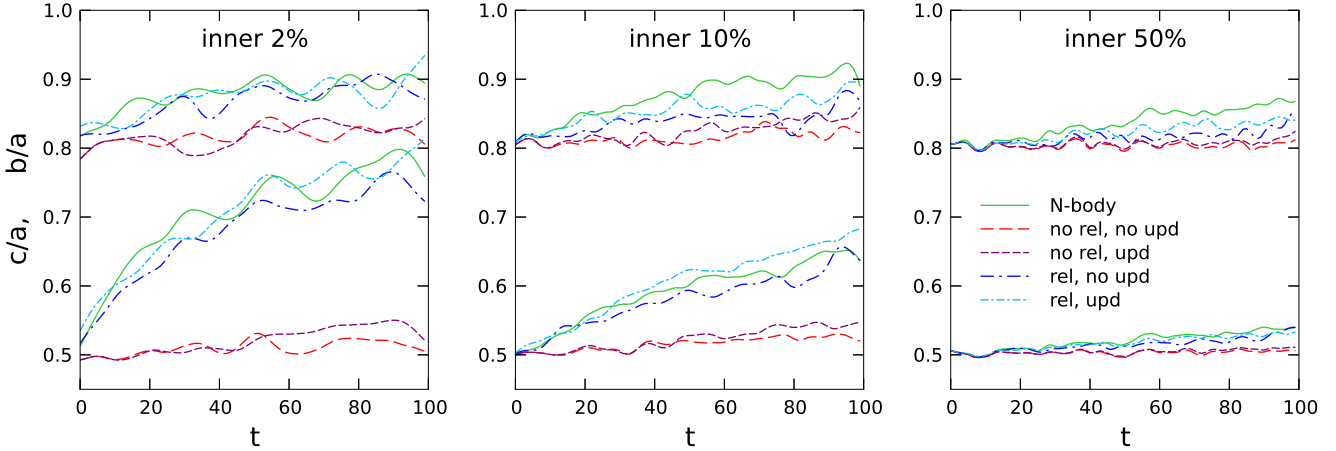


Figure 4. Evolution of shape of a triaxial $\gamma = 1$ Dehnen model with a central black hole of mass $M_{\bullet} = 0.01$ of the total model mass. Three panels display the axis ratios (b/a – intermediate to major and c/a – minor to major) evaluated at a radius containing 2, 10 and 50% of total mass (excluding the black hole). Solid lines are for the N -body simulation ($N = 10^5$), other lines are for the Monte Carlo simulations with or without relaxation and with or without potential update (coefficients of potential expansion recomputed every 10 time units). Clearly, relaxation has a dramatic effect on the evolution of shape towards more sphericity in the central parts of the model, with the rate of evolution similar to that seen in the N -body simulation. The potential update does not seem to have a significant impact; if anything, it accelerates the evolution slightly.

of the total model mass. This was one of the test models for the SMILE code for Schwarzschild (1979) modelling described in Vasiliev (2013, Section 7.1). The simulation was conducted with the ϕ GRAPEch code using $N = 10^5$ particles. It was found that the model evolved towards a somewhat less flattened and less triaxial shape over the timescale of simulation (100 time units). Such evolution is not unexpected in light of previous studies (e.g. Gerhard & Binney 1985; Merritt & Quinlan 1998), although later papers suggested that the evolution may be not as rapid as found earlier (Holley-Bockelman et al. 2002; Poon & Merritt 2004). The driving force behind this shape evolution is thought to be the scattering of chaotic orbits by the central point mass: this would let them more uniformly populate the equipotential surface, which is typically rounder than the equidensity surface. However, the diffusion of chaotic orbits may be greatly facilitated by the graininess of potential (Pogorelov & Kandrup 1999; Kandrup et al. 2000), and very little has been explored on this topic.

We performed simulations of the same system as studied in Vasiliev (2013) with the Monte Carlo code, in several regimes, using a combination of two options: (i) without two-body relaxation or with the stochastic perturbation equivalent to the relaxation rate of an $N = 10^5$ system, and (ii) using a fixed initial potential, or updating the potential every 10 time units (for a total simulation time of 100 time units). We used the iterative method E1 of Zemp et al. (2011) for computing the axis ratios of our models as functions of radius (the same method was used in the previous paper).

Figure 4 shows the evolution of shape for our four runs, together with the one from the N -body simulation. Clearly, in the absence of relaxation the shape does not substantially evolve, regardless of whether we update the potential or keep it fixed. On the other hand, inclusion of relaxation dramatically accelerates the shape evolution in the central

parts of the model, bringing it in good agreement with the results of N -body simulation. This experiment suggests that the evolution of shape can be at least partially attributed to the discreteness noise which accelerates the chaotic diffusion. The substantial reduction of unwanted collisional relaxation offered by the presented Monte Carlo scheme offers new avenues in exploring the interplay between discreteness and chaos, enabling a more robust study of chaotic diffusion and its effect on the galaxy shape (e.g. Vasiliev & Athanassoula 2012).

6 CONCLUSIONS

We have reviewed the existing methods for simulating the evolution of stellar systems driven by the two-body relaxation, and proposed a new variant of Monte Carlo method suitable for studying non-spherical systems. It combines the flexible representation of the smooth average potential in terms of spherical-harmonic expansion (similar to the SCF method of Hernquist & Ostriker 1992) with the Spitzer’s approach to the description of two-body relaxation in terms of local (position-dependent) velocity diffusion coefficients. The orbits of particles are thus evolved on a dynamical timescale, with the two-body interaction between them mediated by the diffusion coefficients computed from a smooth, nearly-stationary distribution function (in a manner similar to the Shapiro’s variant of the Monte Carlo method, but without orbit-averaging). We have shown that the method reproduces some standard evolutionary models, and has a substantially reduced artificial relaxation rate (related to random fluctuations in the potential expansion coefficients) compared to the SCF method. The wall-clock computation time of the Monte Carlo code was within one hour for all simulations discussed in this paper (using a typical multi-core desktop), while some of the N -body simulations took a few days using

high-end GPUs. The RAGA code is made publicly available at <http://td.lpi.ru/~eugvas/raga/>; additionally, its inclusion into the AMUSE framework (Portegies Zwart et al. 2013) is underway.

In the present implementation, the Monte Carlo method has a number of limitations, most of which are not fundamental:

- The Monte Carlo method (in this and other variants, with the possible exception of Spitzer’s original formulation) is not suitable for systems which are not in dynamical equilibrium.
- The fluctuations in velocities (and, hence, energies) of particles are simulated independently from each other, which means that at the end of the Monte Carlo episode the total energy has, in general, a non-zero accumulated deviation. It is corrected by distributing this energy error between all particles, in proportion to their time-averaged energy diffusion coefficient, but the correction is applied to the magnitudes of velocity only. This could in principle bias the dynamics somewhat, but at least avoids much larger errors which occur without any such correction. The total angular momentum of the system is not conserved, but its fluctuations due to discreteness noise are rather small for a reasonable particle number.
- The calculations assumed that all stars have the same mass. This is quite easy to generalize, by allowing each simulation particle to carry a given “token” dynamical mass (which enters the expression (1a) for the drift coefficient), and this mass needs not be related to the actual amount of mass that this particle contributes to the total potential. In other words, we generalize Hénon’s concept of “superstars” by completely separating the notions of dynamical and tracer mass. Likewise, stellar evolution may be accounted for by allowing this token mass to change with time. We note that for all simulations in this paper, we scaled the diffusion coefficients in such a way as to model a system with the number of stars N being the same as the number of particles in the model, but this was done only to facilitate comparison with N -body simulations and is not a restriction of the code.
- We ignored primordial and dynamically formed binaries and their contribution to the energy budget of the system, and did not consider the process of escape of stars. This could be implemented in a similar way to other state-of-the-art codes (e.g. Fregeau et al. 2003; Giersz & Spurzem 2003).
- Stellar collisions in dense galactic nuclei may be accounted for by a scheme similar to Duncan & Shapiro (1983) and Freitag & Benz (2002).
- The discrete nature of mass tracers makes it difficult to simulate a system with high density contrast without resorting to mass refinement schemes. Fortunately, in our implementation, the mass of a particle can be set in an arbitrary way, for instance, creating initial conditions with higher mass resolution where necessary (e.g. Zemp et al. 2008; Zhang & Magorrian 2008). However, if the evolution time is substantially longer than the central relaxation time, particles will tend to mix in energy, erasing the effect of mass refinement. To combat this, an adaptive “creation–annihilation scheme”, such as that employed by Shapiro & Marchant (1978) and Freitag & Benz (2002), could be added to the algorithm. However, this mixing would

also presumably drive the system towards spherical symmetry, so that the benefits of the arbitrary-geometry code would be irrelevant; for systems with longer relaxation times (such as galactic nuclei) the initial mass refinement should suffice.

- The diffusion coefficients are computed under the approximation of a spherically symmetric isotropic distribution function of background stars. This is perhaps the most fundamental limitation, and it means that we may reliably simulate only systems that are not too flattened and not too far from isotropy. It is known that in stellar systems that are at least partially rotationally supported, the two-body relaxation proceeds faster as the velocity dispersion is lower (e.g. Goodman 1983; Sellwood 2013; Šubr & Haas 2014). However, it is possible to adapt the computation of diffusion coefficients for a distribution function that is isotropic in the rotating frame (Einsel & Spurzem 1999).
- Similarly, we did not take into account the processes that are not described by standard two-body relaxation theory, such as resonant relaxation in the vicinity of a massive black hole (Rauch & Tremaine 1996) or non-Gaussian character of energy diffusion at $t \ll T_{\text{rel}}$ (Bar-Or et al. 2013). The proper account of these processes is hindered by the fact that they are not simply described by uncorrelated random walk, and require more sophisticated statistical models (e.g. Madigan et al. 2011). The error introduced by neglecting these effects depends on the question being addressed. For instance, the total rate of capture of stars by a massive black hole is rather weakly influenced by resonant relaxation, as shown by Hopman & Alexander (2006) as well as by our own comparison of direct N -body simulations with the Fokker–Planck models (Vasiliev & Merritt 2013), because the bulk of captured stars come from larger energies that those for which the resonant relaxation is effective. On the other hand, it surely is important for stars very close to the black hole, as are relativistic effects (e.g. Merritt et al. 2011), also ignored in this study.

The possibility of simulating collisional relaxation for stellar systems with arbitrary shape opens up a number of opportunities, especially for studies of elliptical galaxies and galactic nuclei which are otherwise inaccessible to direct N -body simulations with present-day computers:

- Noise is known to enhance the efficiency of chaotic diffusion (e.g. Kandrup et al. 2000), especially in systems with a rich population of sticky chaotic orbits (Habib et al. 1997), such as triaxial Dehnen models (Valluri & Merritt 1998), and has been proposed to improve the phase-space coverage of chaotic orbits in the construction of Schwarzschild models (Siopis & Kandrup 2000). However, very little is known of the implications of noise for the secular evolution of triaxial galaxies which may – or may not, depending on their orbital structure – evolve noticeably away from triaxiality during the Hubble time (Vasiliev & Athanassoula 2012).
- Non-spherical galactic nuclei have been proposed as a way to increase the rate of star captures by a supermassive black hole (Norman & Silk 1983; Gerhard & Binney 1985; Merritt & Poon 2004; Holley-Bockelmann & Sigurdsson 2006), if the triaxiality can persist for the Hubble time. On the other hand, scattering of chaotic orbits by the black hole might destroy or reduce the triaxiality (Merritt & Quinlan 1998; Holley-Bockelman et al. 2002),

and the collisional relaxation increases the rate of diffusion of stars into the black hole even in the axisymmetric potential (Magorrian & Tremaine 1999; Vasiliev & Merritt 2013). The evolution of non-spherical black hole nuclei, including the loss of stars into the black hole and changes in the galaxy shape, is difficult to follow by conventional N -body simulations because of very low relaxation rates in actual galaxies, compared to what can be achieved in the direct simulations. This topic is explored with the new Monte Carlo method in a separate paper (Vasiliev 2014).

- Likewise, the dynamics of binary supermassive black holes is substantially changed in a non-spherical system (Berczik et al. 2006; Preto et al. 2011; Khan et al. 2011, 2013), although an accurate treatment of collisional relaxation in the non-spherical case is even more difficult for a binary black hole (Vasiliev et al. 2014).

- After implementing mass-dependent velocity drift coefficient, it becomes possible to study dynamical friction of not too massive objects (heavier than field stars, but much lighter than the total mass of the model) in non-spherical galaxies (e.g. Binney 1977; Pesce et al. 1992; Cora et al. 2001; Vicari et al. 2007) in a more self-consistent way (including possible feedback on the galaxy shape). A related idea was recently explored by Brockamp et al. (2014), although their generic machinery of basis-set expansion was only applied for the spherical case. Likewise, collisional evolution and mass segregation in galactic nuclei has been mostly studied in the spherical case (Freitag et al. 2006; Alexander & Hopman 2009; Merritt 2010); only a few studies have considered non-spherical nuclei, resulting, for instance, from galactic mergers (e.g. Gualandris & Merritt 2012) or globular cluster inspirals (e.g. Antonini 2014).

- Accurate treatment of escape of stars from globular clusters in a realistic tidal field of a galaxy is non-trivial (Fukushige & Heggie 2000), and it is quite tricky to implement it in a spherical Monte Carlo code (Giersz et al. 2013; Sollima & Mastrobuono-Battisti 2014). More generally, non-spherical globular clusters may present other interesting phenomena to study (e.g. Carpintero et al. 1999).

- By modifying the expressions for diffusion coefficients using a suitable definition of background distribution function of stars (for instance, lifting the assumption of isotropy), it will be possible to study rotating clusters (cf. Einsel & Spurzem 1999; Fiestas & Spurzem 2010, who used axisymmetric Fokker–Planck models).

I warmly thank Douglas Heggie and Mirek Giersz for detailed comments on the early version of the manuscript, and am grateful to the anonymous referee for helpful remarks that improved the presentation. This work was partly supported by the National Aeronautics and Space Administration under grant no. NNX13AG92G.

REFERENCES

- Aarseth S., 1967, in “Les Nouvelles Méthodes de la Dynamique Stellaire”. Editions de CNRS, Paris, p.47
- Alexander T., Hopman C. 2009, *ApJ*, 697, 1861
- Amaro-Seoane P., Freitag M., Spurzem R. 2004, *MNRAS*, 352, 655
- Ahnert K., Mulansky M. 2011, *AIP Conf. Proc.* 1389, 1586
- Antonini F. 2014, *ApJ*, 794, 106
- Antonini F., Merritt D. 2012, *ApJ*, 745, 83
- Athanassoula E., Bosma A., Lambert J.-C., Makino J., 1998, *MNRAS*, 293, 369
- Bahcall J. & Wolf R. 1976, *ApJ*, 209, 214
- Bar-Or B., Kupi G., Alexander T. 2013, *ApJ*, 764, 52
- Baumgardt H., Heggie D., Hut P., Makino J. 2003, *MNRAS*, 341, 247
- Baumgardt H., Makino J., Ebisuzaki T. 2004, *ApJ*, 613, 1133
- Berczik P., Merritt D., Spurzem R., Bischof H. 2006, *ApJ*, 642, L21
- Binney J. 1977, *MNRAS*, 181, 735
- Brockamp M., Küpper A.H.W., Thies I., Baumgardt H., Kroupa P. 2014, *MNRAS*, 441, 150
- Carpintero D., Muzzio J., Wachlin F. 1999, *Celest. Mech. Dyn. Astron.*, 73, 159
- Chang J. S., Cooper G. 1970, *J. Comput. Phys.*, 6, 1
- Chatterjee S., Fregeau J., Umbreit S., Rasio F. 2010, *ApJS*, 204, 15
- Chavanis P.-H. 2013, *A&A*, 556, 93
- Clutton-Brock M., 1973, *Ap&SS*, 23, 55
- Cohn H. 1979, *ApJ*, 234, 1036
- Cohn H. 1980, *ApJ*, 242, 765
- Cohn H., Kulsrud R. 1978, *ApJ*, 226, 1087
- Cora S., Vergne M., Muzzio J. 2001, *ApJ*, 546, 165
- Dehnen W. 1993, *MNRAS*, 265, 250
- Drukier G., Cohn H., Lugger P., Yong H. 1999, *ApJ*, 518, 233
- Duncan M., Shapiro S. 1983, *ApJ*, 268, 565
- Einsel Ch., Spurzem R. 1999, *MNRAS*, 302, 81
- Fiestas J., Spurzem R. 2010, *MNRAS*, 405, 194
- Fregeau J., Rasio F. 2007, *ApJ*, 658, 1047
- Fregeau J., Gürkan M.A., Joshi K., Rasio F. 2003, *ApJ*, 593, 772
- Freitag M., Benz W. 2001, *A&A*, 375, 711
- Freitag M., Benz W. 2002, *A&A*, 394, 345
- Freitag M., Amaro-Seoane P., Kalogera V. 2006, *ApJ*, 649, 91
- Fujii M., Iwasawa M., Funato Y., Makino J. 2011, *PASJ*, 59, 1095
- Fukushige T., Heggie D. 2000, *MNRAS*, 318, 753
- Gaburov E., Harfst S., Portegies Zwart S. 2009, *New Astron.*, 14, 630
- Gerhard O., Binney J. 1985, *MNRAS*, 216, 467
- Giersz M. 1998, *MNRAS*, 298, 1239
- Giersz M., Heggie D. 1994, *MNRAS*, 268, 257
- Giersz M., Spurzem R. 2003, *MNRAS*, 343, 781
- Giersz M., Heggie D., Hurley J., Hypki A. 2013, *MNRAS*, 431, 2184
- Goodman J. 1983, PhD thesis, Princeton Univ.
- Green P., Silverman B., 1994, *Nonparametric regression and generalized linear models*. Chapman&Hall, London
- Gualandris A., Merritt D. 2012, *ApJ*, 744, 74
- Habib S., Kandrup H., Mahon M. 1997, *ApJ*, 480, 155
- Hairer E., Nørsett S., Wanner G., 1993, *Solving ordinary differential equations*. Springer-Verlag, Berlin
- Hamers A., Portegies Zwart S., Merritt D. 2014, *MNRAS*, 443, 355
- Harfst S., Gualandris A., Merritt D., Spurzem R., Portegies Zwart S., Berczik P. 2007, *New Astron.*, 12, 357
- Harfst S., Gualandris A., Merritt D., Mikkola S. 2008, *MNRAS*, 389, 2

- Heggie D., Hut P. 2003, The gravitational million-body problem. Cambridge Univ. press, Cambridge
- Hemsendorf M., Sigurdsson S., Spurzem R. 2002, ApJ, 581, 1256
- Hénon M., 1967, in “Les Nouvelles Méthodes de la Dynamique Stellaire”. Editions de CNRS, Paris, p.91
- Hénon M., 1971, Ap&SS, 13, 284
- Hénon M., 1971, Ap&SS, 14, 151
- Hernquist L., Barnes J. 1990, ApJ, 349, 562
- Hernquist L., Ostriker J., 1992, ApJ, 386, 375
- Holley-Bockelmann K., Mihos J., Sigurdsson S., Hernquist L., Norman C. 2002, ApJ, 567, 817
- Holley-Bockelmann K., Sigurdsson S. 2006, arXiv:astro-ph/0601520
- Hopmen C. 2009, ApJ, 700, 1933
- Hopman C., Alexander T. 2006, ApJ, 645, 1152
- Hurley J., Pols O., Tout Ch. 2000, MNRAS, 315, 543
- Hurley J., Tout Ch., Pols O. 2002, MNRAS, 329, 897
- Hypki A., Giersz M. 2013, MNRAS, 429, 1221
- Johnston K., Sigurdsson S., Hernquist L. 1999, MNRAS, 302, 771
- Joshi K., Rasio F., Portegies Zwart S. 2000, ApJ, 540, 969
- Kandrup H., Pogorelov I., Sideris I. 2000, MNRAS, 311, 719
- Khan F. M., Just A., Merritt D. 2011, ApJ, 732, 89
- Khan F. M., Holley-Bockelmann K., Berczik P., Just A. 2013, ApJ, 773, 100
- Kloeden P., Platen E., 1995, Numerical solution of stochastic differential equations. Springer-Verlag, Berlin
- Kocsis B., Tremaine S. 2014, MNRAS (submitted); arXiv:1406.1178
- Louis P., Spurzem R. 1991, MNRAS, 251, 408
- Madigan A.-M., Hopman C., Levin Y. 2011, ApJ, 738, 99
- Magorrian J., Tremaine S. 1999, MNRAS, 309, 447
- Makino J. 1996, ApJ, 471, 796
- Marchant A., Shapiro S. 1979, ApJ, 234, 317
- Marchant A., Shapiro S. 1980, ApJ, 239, 685
- McMillan S., Aarseth S. 1993, ApJ, 414, 200
- McMillan S., Lightman A. 1984, ApJ, 283, 801
- Meiron Y., Li B., Holley-Bockelmann K., Spurzem R. 2014, ApJ, 792, 98
- Merritt D. 1996, AJ, 111, 2462
- Merritt D. 2009, ApJ, 694, 959
- Merritt D. 2010, ApJ, 718, 739
- Merritt D. 2013, Dynamics and evolution of galactic nuclei. Princeton Univ. Press, Princeton, NJ
- Merritt D., Poon M. 2004, ApJ, 606, 788
- Merritt D., Quinlan G. 1998, ApJ, 498, 625
- Merritt, D., Szell, A. 2006, ApJ, 648, 890
- Merritt D., Alexander T., Mikkola S., Will C. 2011, Phys. Rev. D, 84, 044024
- Norman C., Silk J. 1983, ApJ, 266, 502
- Oshino S., Funato Y., Makino J. 2011, PASJ, 63, 881
- Park B., Petrosian V. 1996, ApJ Suppl., 103, 255
- Pattabiraman B., Umbreit S., Liao W.-K., Choudhary A., Kalogera V., Memik G., Rasio F. 2013, ApJS, 204, 15
- Pelupessy I., van Elteren A., de Vries N., McMillan S., Drost N., Portegies Zwart S. 2013, A&A, 557, A84
- Pesce E., Capuzzo-Dolcetta R., Vietri M. 1992, MNRAS, 254, 466
- Pogorelov I., Kandrup H. 1999, Phys. Rev. E, 60, 1567
- Poon M. Y., Merritt D. 2004, ApJ, 606, 774
- Portegies Zwart S., McMillan S., van Elteren E., Pelupessy I., de Vries N. 2013, Comput. Phys. Commun., 184, 456
- Preto M., Merritt D., Spurzem R. 2004, ApJ, 613, L109
- Preto M., Berentzen I., Berczik P., Spurzem R. 2011, ApJ, 732, L26
- Quinlan G. 1996, New Astron., 1, 255
- Rauch K., Tremaine S. 1996, New Astron., 1, 149
- Schwarzschild M. 1979, ApJ, 232, 236
- Sellwood J. 2013, ApJ, 769, L24
- Shapiro S. 1985, in Goodman J. & Hut P., eds, Proc. IAU Symp. 113, Dynamics of Star Clusters, p.373
- Shapiro S., Marchant A. 1978, ApJ, 225, 603
- Siopis Ch., Kandrup H. 2000, MNRAS, 319, 43
- Sollima A., Mastrobuono-Battisti A. 2014, MNRAS, 443, 3513
- Spitzer L. 1975, in Hayli A., ed., Proc. IAU Symp. 69, Dynamics of Stellar Systems, p.3
- Spitzer L., Hart, M. 1971, ApJ, 164, 399
- Spitzer L., Mathieu R. 1980, ApJ, 241, 618
- Spitzer L., Shapiro S. 1972, ApJ, 173, 529
- Spitzer L., Shull J. 1975, ApJ, 200, 339
- Spitzer L., Thuan T. 1972, ApJ, 175, 31
- Spurzem R., Giersz M. 1996, MNRAS, 283, 805
- Stodólkiewicz J. 1982, Acta Astron., 32, 63
- Stodólkiewicz J. 1986, Acta Astron., 36, 19
- Šubr L., Haas J. 2014, ApJ, 786, 121
- Szell A., Merritt D., Kevrekidis I. 2005, Phys. Rev. Lett. 95, 081102
- Takahashi K. 1993, PASJ, 45, 233
- Takahashi K. 1995, PASJ, 47, 561
- Theis Ch. 1998, A&A, 330, 1180
- Theuns T. 1996, MNRAS, 279, 827
- Touma J., Tremaine S., Kazandjian M. 2009, MNRAS, 394, 1085
- Tremaine S., Richstone D., Byun Y.-I., Dressler, A., Faber, S., Grillmair, C., Kormendy, J., Lauer, T., 1994, AJ, 107, 634
- Umbreit S., Fregeau J., Chatterjee S., Rasio F. 2012, ApJ, 750, 31
- Valluri M., Merritt D. 1998, ApJ, 506, 686
- van Albada T., van Gorkom J., 1977, A&A, 54, 121
- Vasiliev E. 2013, MNRAS, 434, 3174
- Vasiliev E. 2014, Class. Quantum Grav., 31, 244002
- Vasiliev E., Antonini F., Merritt D. 2014, ApJ, 785, 163
- Vasiliev E., Athanassoula E., 2012, MNRAS, 419, 3268
- Vasiliev E., Merritt D. 2013, ApJ, 774, 87
- Vicari A., Capuzzo-Dolcetta A., Merritt D. 2007, ApJ, 662, 797
- Weinberg M. 1996, ApJ, 470, 715
- Weinberg M., Katz N., 2007, MNRAS, 375, 425
- Zemp M., Moore B., Stadel J., Carollo M., Madau P., 2008, MNRAS, 386, 1543
- Zemp M., Gnedin O., Gnedin N., Kravtsov A., 2011, ApJS, 197, 30
- Zhang M., Magorrian J., 2008, MNRAS, 387, 1719